ESC European Society of Cardiology

European Heart Journal - Cardiovascular Imaging (2019) **20**, 209–217
doi:10.1093/ehjci/jey069

Proximal pulmonary vascular stiffness as a prognostic factor in children with pulmonary arterial hypertension

Richard M. Friesen[1,2*†], Michal Schäfer[1,3†], D. Dunbar Ivy[1], Steven H. Abman[4], Kurt Stenmark[5], Lorna P. Browne[6], Alex J. Barker[7], Kendall S. Hunter[1,3], and Uyen Truong[1]

[1]Division of Cardiology, Heart Institute, Children's Hospital Colorado, University of Colorado Denver, Anschutz Medical Campus, 13123 E 16th Avenue, Aurora, CO 80045-2560, USA; [2]Department of Critical Care, Seattle Children's Hospital, University of Washington, 4800 Sand Point Way NE, Seattle, WA 98105, USA; [3]Department of Bioengineering, College of Engineering and Applied Sciences, University of Colorado Denver, Anschutz Medical Campus, 12705 E. Montview Ave, Aurora, CO 80045, USA; [4]Division of Pulmonology, Breathing Institute, Children's Hospital Colorado, University of Colorado Denver, Anschutz Medical Campus, 13123 E 16th Avenue, Aurora, CO 80045-2560, USA; [5]Developmental Lung Biology and Cardiovascular Pulmonary Research Laboratories, University of Colorado Denver, Anschutz Medical Campus, 12700 E 19th Ave, Box B131. Aurora, CO 80045, USA; [6]Department of Radiology, Children's Hospital Colorado, University of Colorado Denver, Anschutz Medical Campus, 13123 E 16th Avenue, Aurora, CO 80045-2560, USA; and [7]Department of Radiology, Feinberg School of Medicine, Northwestern University, 737 N Michigan Ave, Suite 1600, Chicago, IL 60611, USA

Received 7 July 2017; editorial decision 17 April 2018; accepted 23 April 2018; online publish-ahead-of-print 16 May 2018

Aims Main pulmonary artery (MPA) stiffness and abnormal flow haemodynamics in pulmonary arterial hypertension (PAH) are strongly associated with elevated right ventricular (RV) afterload and associated with disease severity and poor clinical outcomes in adults with PAH. However, the long-term effects of MPA stiffness on RV function in children with PAH remain poorly understood. This study is the first comprehensive evaluation of MPA stiffness in children with PAH, delineating the mechanistic relationship between flow haemodynamics and MPA stiffness as well as the prognostic ability of these measures regarding clinical outcomes.

Methods and results Fifty-six children diagnosed with PAH underwent baseline cardiac magnetic resonance (CMR) acquisition and were compared with 23 control subjects. MPA stiffness and wall shear stress (WSS) were evaluated using phase contrast CMR and were evaluated for prognostic potential along with standard RV volumetric and functional indices. Pulse wave velocity (PWV) was significantly increased (2.8 m/s vs. 1.4 m/s, $P < 0.0001$) and relative area change (RAC) was decreased (25% vs. 37%, $P < 0.0001$) in the PAH group, correlating with metrics of RV performance. Decreased WSS was associated with a decrease in RAC over time ($r = 0.679$, $P < 0.001$). For each unit increase in PWV, there was approximately a 3.2-fold increase in having a moderate clinical event.

Conclusion MPA stiffness assessed by non-invasive CMR was increased in children with PAH and correlated with RV performance, suggesting that MPA stiffness is a major contribution to RV dysfunction. PWV is predictive of moderate clinical outcomes, and may be a useful prognostic marker of disease activity in children with PAH.

Keywords Paediatrics • Pulmonary hypertension • Cardiac magnetic resonance • Vascular stiffness

Introduction

Proximal pulmonary vascular stiffness and abnormal flow haemodynamics are increasingly recognized as being strongly associated with elevated right ventricular (RV) afterload in both children and adults with pulmonary arterial hypertension (PAH).[1–5] Non-invasive surrogate indices of main pulmonary arterial (MPA) stiffness have previously been shown to reflect disease severity, catheterization-derived haemodynamics, and most importantly, poor clinical outcomes in heterogeneous adult PAH populations.[6–8] However, the prognostic

* Corresponding author. Tel: +1 (206) 987-5391; Fax: +1 (206) 987-3866. E-mail: richard.friesen@seattlechildrens.org

† These authors are first co-authors.

utility of indices of MPA stiffness in paediatric PAH is unknown. Furthermore, the exact interplay between proximal pulmonary vascular stiffness and abnormal flow haemodynamics in the proximal pulmonary arterial conduit is still unknown despite increasing evidence supporting a key role of flow-mediated vascular remodelling in disease progression of the pulmonary and systemic circulations.[9,10]

Characterization of pulmonary vascular stiffness in children is a challenging task due to the invasiveness of right heart catheterization, heterogeneity of congenital heart defects (CHDs) commonly associated with paediatric PAH, and limited number of studies that follow paediatric patients through transition to adult PAH programmes.[11,12] While not direct measurements of intrinsic vascular properties, non-invasive markers of pulmonary vascular stiffness may obviate some of these challenges. Using non-invasive cardiac magnetic resonance (CMR), we have previously reported that reduced relative area change (RAC) and haemodynamic wall shear stress (WSS) in large pulmonary arteries are strongly associated with disease severity in children.[13,14] Elevated WSS is typically associated with systemic vasculopathies, and consequently with endothelial damage and extracellular matrix degradation.[10,15] However, decreased WSS is commonly present in the proximal pulmonary arteries of patients with PAH, which likely promotes a pro-inflammatory endothelial cell phenotype, smooth muscle cell proliferation, and inflammatory cell infiltration.[16,17] The typically dilated proximal pulmonary vasculature is prone to flow mediated augmentation of vascular stiffness, consequently leading to additional rise in RV afterload.

To further and more comprehensively investigate this pathophysiological process in children with PAH, we evaluated serial changes in pulmonary flow haemodynamics and MPA stiffness and sought to determine the clinically prognostic potential of MPA stiffness indices. We hypothesized that non-invasively derived markers of vascular stiffness, pulse wave velocity (PWV) and RAC, will change, in a longitudinal fashion, with shear haemodynamics and will predict clinical outcomes in children with PAH. Better understanding of the interplay between flow haemodynamics and vascular stiffness with respect to clinical prognostics may provide more information to guide therapeutic management and pharmacological targeting of PAH.

Methods

This study was approved by the Colorado Multi-Institutional Review Board, and all subjects provided written informed consent. Patients with PAH seen by the Pulmonary Hypertension Clinic at Children's Hospital Colorado who underwent comprehensive CMR from December 2007 to August 2016 were included. The initial diagnosis of PAH was established after evaluation by our Pulmonary Hypertension Program, which included echocardiograms and a prior cardiac catheterization, according to accepted guidelines.[3,18] World Health Organization functional class (WHO-FC) was evaluated during the initial visit and all subsequent clinical visits at the Pulmonary Hypertension clinic with the time interval between individual follow-ups ranging between 3 weeks to 6 months. Exclusion criteria included (i) present pulmonary valve or pulmonary arterial stenosis determined by CMR or echocardiography, (ii) patients with absent primary pulmonary branch, and (iii) previous surgical intervention on the pulmonary vasculature involving artificial material, such as right ventricle to pulmonary arterial conduits. Control subjects were prospectively recruited through campus advertisement and were included if they did not have any known underlying cardiac, pulmonary, or systemic disease. Catheterization-derived data from the chronologically closest study to the CMR was used for this study.

CMR acquisition

The acquisition protocol was performed as described previously.[13,14] A gradient echo electrocardiogram gated sequence was applied to obtain tissue intensity and phase velocity maps using a 1.5 or 3.0 Tesla magnet (Magnetom Avanto, Siemens Medical Solutions, Erlangen, Germany; Ingenia, Philips Medical Systems, Best, The Netherlands). The flow haemodynamic parameters were measured using phase-contrast CMR, in the mid-section of the MPA in orthogonal fashion confirmed by corresponding angiogram (*Figure 1*). The free breathing phase-contrast CMR with Cartesian encoding and retrospective sorting had a temporal

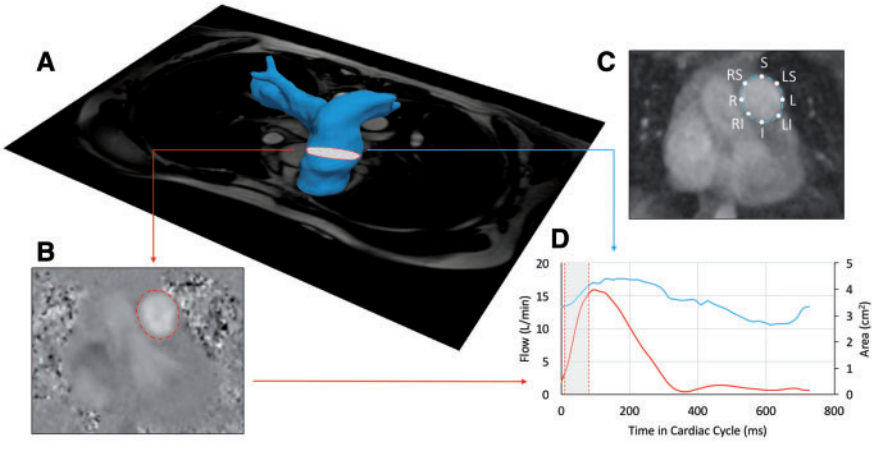

Figure 1 (*A*) Magnetic resonance angiography reconstructed MPA with superimposed plane of phase-contrast CMR was applied to ensure the universally applied location for flow and stiffness analysis. (*B*) Exemplary phase-contrast image with the segmentation line derived from corresponding magnitude image. (*C*) Magnitude image with location specific labelled point of WSS analysis. (*D*) Created flow and area waveforms with highlighted region of the PWV analysis at the early ejection phase.

resolution of 14–28 ms with 30–50 phases, echo times of 2.2–3.5 ms, matrix: 160 × 256, flip angle of 25° with 100% of the k-space sampled without any further temporal resolution reconstruction algorithms being applied. Depending on patient size and field of view (128–225 × 210–360 mm), the cross-sectional pixel resolution was 0.82 × 0.82–1.56 × 1.56 mm^2 with a slice thickness of 5 mm. Resulting acquisition time varied between 2 and 3 min, depending upon heart rate. Velocity encoding values were adjusted according to the maximum velocities encountered during scout sequences to avoid aliasing artefact (typical values ranged from 100 to 150 cm/s) per consensus recommendation.[19]

RV dimensional analysis was performed through standard short-axis images with coverage of the ventricles from base to apex as described previously.[14] RV volume and cardiac output were indexed for body surface area (BSA). In addition to standard RV volumetric and functional metrics we calculated RV ventricular-vascular coupling ratio (VVCR) using simplified CMR method (end-systolic volume/stroke volume).[20]

Pulmonary vascular stiffness analysis

To characterize MPA stiffness, we used measures of flow-area (dQ/dA) that are applicable for proximal regions of great vessels, as described previously.[21,22] Flow and area change waveforms were analysed from time-frame segmented respective phase-contrast and magnitude images (Matlab Program; Mathworks, Inc., Natick, MA, USA). To limit the effect from backward wave reflections, we sampled data points for PWV evaluation only during the early phase of ejection and excluded data points suggestive of early reflection, which would have created an upstroke notch within the flow curve or when the flow-area curve revealed a plateau at the end of the upstroke phase (*Figure 1*). For the final computation of dQ/dA slope representing PWV, 4–6 data points were needed to ensure reliable linear fit.[21–23] The RAC was computed from the segmented magnitude images as $(A_{max}\text{-}A_{min})/A_{max}$*100%.

Shear haemodynamics

The through-plane WSS at the MPA plane was computed as shown previously from eight points along the MPA lumen.[13,22] Specifically, WSS was sampled at 45° increments along the MPA lumen for localized position specific analysis. These positions were denoted to reflect anatomical location within the MPA plane as S, LS, RS, L, R, RI, LI, and I, representing the superior, left-superior, right-superior, left, right, right-inferior, left-inferior, and inferior MPA lumen locations (*Figure 1*). From the WSS waveform, maximum systolic WSS (WSS_{max}), time-averaged WSS (WSS_{TA}), and oscillatory shear index (OSI) were collected. OSI, previously described by Ku *et al.*[24] is descriptive of the deviation of shear stress from its principle direction. The OSI describes the directional uniformity of WSS which can be comprised particularly in the presence of chaotic and turbulent flow. Highly oscillatory shear described by high OSI values is associated with poor endothelial function and vascular remodelling.[14,25] Additional parameters were sampled from patient specific flow waveforms: maximum flow (Q_{max}), maximum velocity (V_{max}), maximum systolic diameter (D_{max}).

Statistical analysis

Analyses were performed in JMP (version 13.1 or higher; SAS Institute, Cary, NC, USA). Variables were checked for the distributional assumption of normality using normal plots, in addition to Kolmogorov–Smirnov and Shapiro–Wilks tests. Variables that were positively skewed (e.g. PWV, OSI, VVCR) were natural log-transformed for the correlative analyses. Demographic and clinical characteristics among children with and without PAH were compared using student *t*-test for normally distributed continuous variables, Wilcoxon-rank sum test for non-normally distributed variables, and χ^2 for categorical variables. Additional group comparisons were performed using Kruskal–Wallis or one-way ANOVA tests between the PAH specific WHO-FC groups and PAH clinical categories. Generalized linear regression models were used to examine association between the MPA stiffness (PWV and RAC) and RV volumetric and functional indices and were adjusted for age, BSA, and sex.

To investigate the relationship between WSS and MPA stiffness over time, a random coefficient model with an intercept and slope fit for each patient with at least two CMR measurements was used as described previously.[26] In addition, a bivariate version of the random coefficients model was applied to investigate whether the trends in WSS over time are associated with changes of MPA stiffness indices. This modelling approach is achieved by simultaneously fitting two univariate mixed effects models, one for each outcome, and specifying a joint multivariate distribution on the random effects. A benefit of this method is that it does not require the outcomes to be measured at the same time.

All MPA and RV characteristics were considered for survival univariate analysis. Univariate Cox proportional hazards analysis was applied to assess the predictive ability of RV and MPA specific variables in all 57 PH patients. Two types of composite outcomes were considered for prognostic analysis. Composite severe outcomes were defined as death, lung transplantation, initiation of intravenous or subcutaneous prostacyclin therapy, clinically indicated atrial septostomy, or need for a Pott's shunt. Composite moderate outcomes were defined by an escalation in WHO-FC, PAH related hospitalization, syncopal event, or haemoptysis. For variables that were found to be significantly associated with survival univariate analysis, Kaplan–Meier survival curves were constructed with specific log-rank test with the population divided by receiver operating characteristics to find the most optimal cut-off values. All patients were followed up to the particular event or the end of the study (August 2016). Significance was based on an α-level of 0.05.

Results

Comprehensive patient characteristics and baseline haemodynamics are summarized in *Table 1*. Fifty-seven patients (average age, 12.1 ± 5.5 years; range 1.5–18.1 years) with baseline CMR acquisition underwent successful MPA stiffness and shear evaluation, and 21 patients had two or more follow-up CMR acquisitions at a mean interval of 3.5 years (range 0.6–6 years). Twenty-three patients had idiopathic PAH, 22 patients had PAH associated with CHD, and 14 had PAH due to other causes. Specific CHD lesions included atrial septal defect ($n = 7$), ventricular septal defect ($n = 6$), atrioventricular septal defect ($n = 2$), coarctation of the aorta ($n = 2$), patent ductus arteriosus ($n = 3$), partially anomalous pulmonary venous return ($n = 1$), transposition of great arteries ($n = 1$), and pulmonary vein stenosis ($n = 1$) with all defects being post repair. Twelve patients were classified within WHO-FC I, 29 subjects as WHO-FC II, 11 subjects as WHO-FC III, and 6 subjects with WHO-FC IV. At the time of initial CMR acquisition, all patients were receiving PAH therapy (40 phosphodiesterase-5 inhibitors, 26 endothelin receptor antagonists, and 25 prostanoid derivatives). 28 patients were receiving monotherapy, and 16 had dual combination therapy, and 13 were receiving triple combination therapy. Catheterization-derived mean pulmonary arterial pressure was 44 ± 17 mmHg with a pulmonary vascular resistance index of 9 ± 6 Wood units*m^2. The median time between catheterization and CMR acquisition was 132 days (range 0–218 days). Comparison of standard RV volumetric measures between PAH and control populations revealed significantly elevated

Table 1 Patient characteristics and baseline haemodynamics

	PAH ($n = 57$)	Control ($n = 23$)	*P*-value
Age (years)	12.1 ± 5.5	13.1 ± 3.7	0.4021
Sex (%)	54	52	0.5136
BSA (m^2)	1.28 ± 0.42	1.35 ± 0.30	0.4248
WHO-FC			
I	12 (21)		
II	29 (51)		
III	11 (19)		
IV	6 (10)		
IPAH	23 (40)		
CHD	22 (38)		
Others	14 (24)		
PDE5i	40 (70)		
ERA	26 (46)		
Prostacyclin	25 (44)		
mPAP (mmHg)	44 ± 17		
PVRi (WU/m^2)	9 ± 6		
RVEDVi (mL/m^2)	122 ± 47	87 ± 13	<0.0001
RVESVi (mL/m^2)	69 ± 45	37 ± 8	<0.0001
SVi (mL/m^2)	53 ± 14	51 ± 8	0.4726
EF (%)	46 ± 12	58 ± 5	<0.0001
VVCR	1.33 ± 0.75	0.74 ± 0.16	0.0005
CI ($L/min/m^2$)	4.1 ± 1.8	3.6 ± 0.8	0.1241
HR	74 ± 24	70 ± 10	0.3819

Data are reported as *n* (%) and mean ± SD.
CHD, congenital heart disease; CI, cardiac index; EDVi, end-diastolic volume index; EF, ejection fraction; ERA, endothelin receptor antagonists; ESVi, end-systolic volume index; HR, heart rate; IPAH, idiopathic pulmonary hypertension; mPAP, mean pulmonary arterial pressure; PDE5i, phosphodiesterase-5 inhibitors; PVRi, pulmonary vascular resistance index; SVi, stroke volume index; VVCR, ventricular-vascular coupling ratio; WHO-FC, World Health Organization functional class.

indexed end-diastolic and end-systolic volumes in the PAH group (both $P < 0.0001$). Furthermore, the RV ejection fraction was significantly decreased in PAH group ($P < 0.0001$) whereas the VVCR was significantly elevated ($P = 0.0005$) in the same group. Indexed stroke volume, cardiac index, and heart rate were similar between PAH and control groups.

Baseline MPA stiffness and WSS analysis

The haemodynamic and MPA stiffness analysis is summarized in *Table 2*. The baseline PWV was significantly increased in the PAH group (2.8 m/s vs. 1.4 m/s, $P < 0.0001$) and correspondingly RAC was significantly depressed in the same group (25% vs. 37%, $P < 0.0001$). Representative PWV analysis with corresponding flow and area waveforms is depicted in *Figure 2*. There was no intergroup variability in PWV between different WHO-FC groups (*Figure 3A*). Similarly, we did not observe any differences in PWV between APAH-CHD or IPAH (*Figure 3B*). Baseline shear haemodynamic analysis revealed decreased WSS_{max} and WSS_{TA} in PAH patients (both $P < 0.0001$). The OSI was significantly increased in the PAH population ($P = 0.0001$). Regional WSS_{max} distribution along the MPA lumen for

Table 2 Main pulmonary artery characteristics

	PAH ($n = 57$)	Control ($n = 23$)	*P*-value
WSS_{max} ($dyne/cm^2$)	4.2 ± 2.2	6.3 ± 1.9	<0.0001
WSS_{TA} ($dyne/cm^2$)	0.9 ± 0.5	1.8 ± 0.6	<0.0001
OSI	0.020 (0.017–0.067)	0.007 (0.001–0.010)	0.0001
Q_{max} (L/min)	17.2 ± 7.2	15.2 ± 3.7	0.1577
V_{max} (cm/s)	80 ± 29	79 ± 18	0.886
D_{max} (cm)	3.1 ± 0.6	2.6 ± 0.3	<0.0001
D_{min} (cm)	2.8 ± 0.6	2.0 ± 0.8	<0.001
RAC (%)	25 ± 11	37 ± 9	<0.0001
PWV (m/s)	2.8 (1.9–4.2)	1.4 (1.3–1.8)	<0.0001

Data are reported as mean ± SD or median with interquartile range.
D_{max}, maximum diameter; OSI, oscillatory shear index; PWV, pulse wave velocity; Q_{max}, maximum flow; RAC, relative area change; V_{max}, maximum velocity; WSS_{max}, maximum systolic wall shear stress; WSSTA, time-averaged wall shear stress.

control and PAH is depicted in *Figure 4*. The WSS_{max} was significantly decreased in all considered anatomical points, except at the inferior aspect of the MPA. The major WSS determinants Q_{max}, V_{max}, and D_{max} revealed variability between PAH and control groups only in D_{max} (3.1 cm vs. 2.6 cm, $P < 0.0001$). The baseline correlations between stiffness markers (PWV and RAC) and RV volumetric and functional indices are summarized in *Table 3*. Both PWV and RAC correlated significantly with ejection fraction, indexed RV end-diastolic and end-systolic volumes, and VVCR (all $P < 0.001$).

Longitudinal MPA stiffness and WSS analysis

The bivariate random coefficient model was applied to estimate and correlate random slopes of MPA stiffness indices with WSS_{max} to investigate the mechanism of shear mediated vascular remodelling (*Figure 5*). The average time between two CMR acquisitions was 3.5 years (range 0.6–6 years). Trends in WSS_{max} were significantly correlated with RAC (R value = 0.679, $P = 0.0007$). However, the relationship in trends between the WSS_{max} and PWV failed to reveal significant relationship (R value = -0.359, $P = 0.1101$).

Predictive analysis

With respect to severe clinical outcomes, the average follow-up time was 2.2 years (range 0.2–7.4 years) in which three patients died, one underwent lung transplantation, six were initiated on intravenous or subcutaneous prostanoid therapy, two received clinically indicated atrial septostomy, and one underwent a Pott's shunt. For the moderate clinical outcomes, the average follow-up time was 2.1 years (range 0.2–8.1 years) during which 20 patients had worsening of WHO-FC, 4 patients experienced syncopal event during clinical visits, three patients had to be hospitalized due to PAH related causes, and one patient experienced haemoptysis. The univariate proportional hazard analysis is summarized in *Table 4*. From all considered MPA and RV specific metrics, only the PWV was shown to have a prognostic potential toward moderate clinical outcomes. For each unit increase in

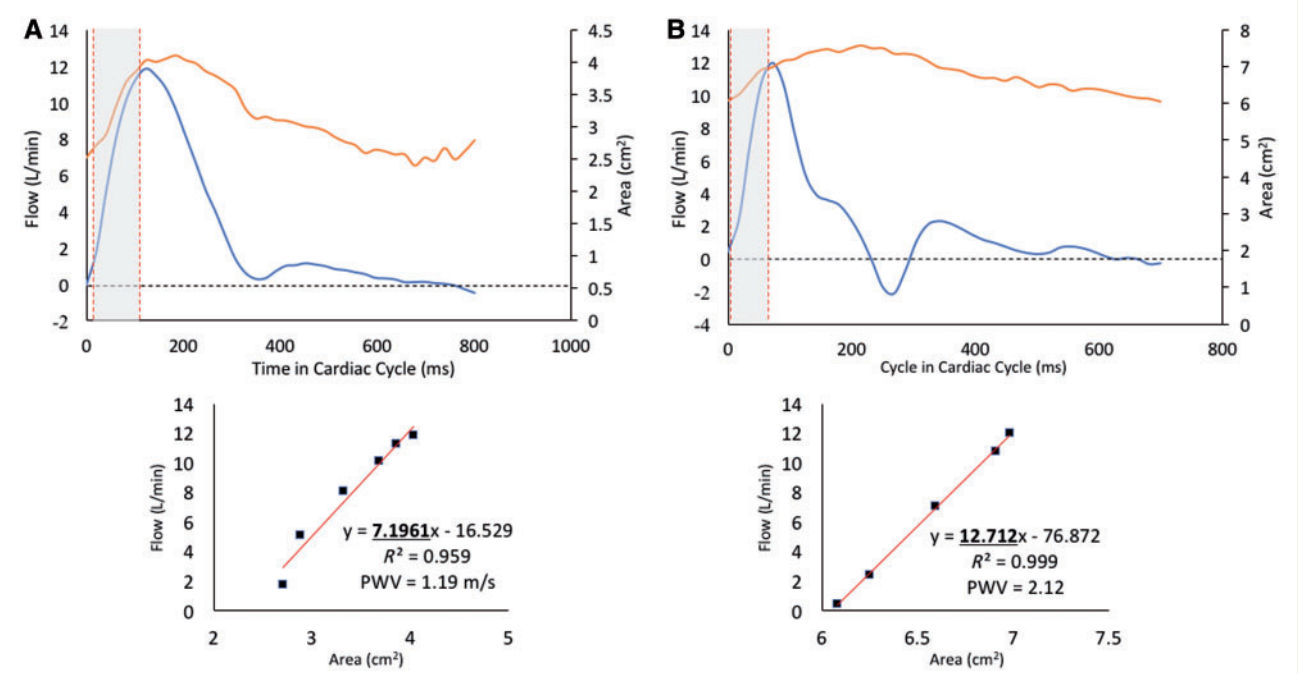

Figure 2 (*A*) Representative control flow haemodynamic waveform with corresponding PWV analysis depicted by linear fit between the flow and area data points during systolic upstroke. (*B*) Representative PAH case depicts typical characteristics of MPA stiffness, including presence of down-stroke notch and backward post-systolic flow.

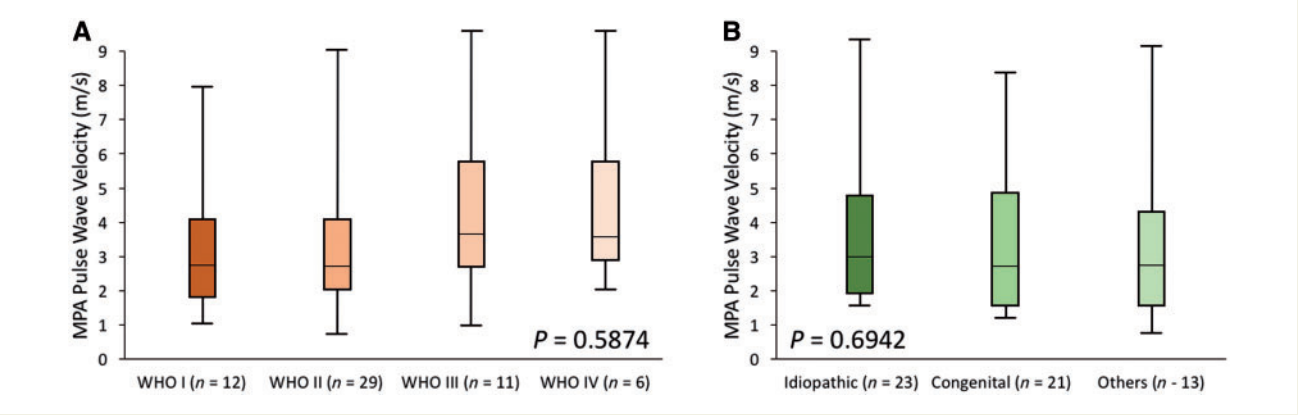

Figure 3 (*A*) Intergroup analysis between different WHO-FC categories did not reveal any variability between considered groups. (*B*) Similarly no intergroup variability existed among different PAH categories. *P*-values are derived Kruskal–Wallis analysis.

PWV, there was approximately a 3.2-fold increase in having a moderate clinical event. The corresponding Kaplan–Meier plot is depicted in *Figure 6* with the receiver operating cut-off value of 2.3 m/s. None of the considered metrics showed potential toward predicting severe clinical event.

Discussion

In this study, we have shown that non-invasive markers of proximal pulmonary vascular stiffness are significantly elevated in the paediatric PAH population, that stiffness metrics representing additional RV afterload are related to RV size and function, and that progression in stiffness could be associated with changes in flow haemodynamic forces acting on the vessel wall. Furthermore, we found that stiffness measured in the MPA can be predictive of moderate clinical events. While the stiffness of proximal pulmonary conduit vessels has been described in studies considering heterogeneous PAH populations,[8,27] this is the first study to demonstrate the potential prognostic utility of non-invasive and comprehensive evaluations of MPA stiffness in children with PAH.

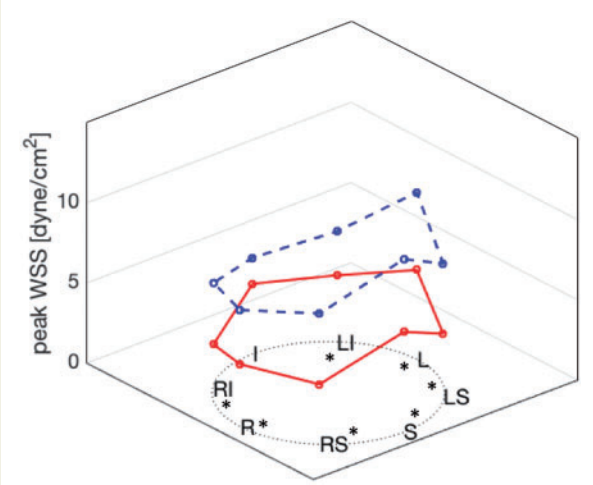

Figure 4 Regional WSS_{max} distribution comparison between controls (blue dashed line) and PAH group (red line). The WSS_{max} was significantly lowered along the entire aspect of the MPA lumen except at the inferior portion of the vessel.

Table 3 RV correlations with measures of MPA stiffness

	PWV (m/s)		RAC (%)	
EF	-0.120 ± 0.018, 0.657	<0.0001	0.508 ± 0.112, 0.515	<0.0001
VVCR[a]	3.05 ± 0.45, 0.662	<0.0001	-12.5 ± 2.6, 0.532	<0.0001
CI	0.038 ± 0.159, 0.202	0.8114	0.383 ± 0.841, 0.206	0.658
EDVi	0.028 ± 0.005, 0.595	<0.0001	-0.119 ± 0.030, 0.467	0.0002
ESVi	0.037 ± 0.005, 0.691	<0.0001	-0.147 ± 0.031, 0.524	<0.0001
SVi	-0.16 ± 0.018, 0.226	0.3874	0.090 ± 0.011, 0.2110	0.4211

Data are reported as beta coefficients ± SEM, *R*-value and *P*-values.
[a]Parameters were log transformed. All correlations are adjusted for age, sex, and BSA.
CI, cardiac index; EDVi, end-diastolic volume index; EF, ejection fraction; ESVi, end-systolic volume index; PWV, pulse wave velocity; RAC, relative area change; SVi, stroke volume index; VVCR, ventricular-vascular coupling ratio.

MPA stiffness in paediatric PAH

In our previous work, we have described significantly reduced WSS metrics and RAC in smaller paediatric PAH populations.[13,14] However, RAC can be considered a simplified metric of MPA stiffness independent of pulse pressure, whereas PWV is considered gold-standard non-invasive index of vascular stiffness.[23] PWV is specifically applicable for vessel stiffness analysis given that considerable wall remodelling may occur prior to alterations in vessel geometry. Additionally, PWV was investigated in this study using flow-area method, which enables region and plane specific analysis, which should be considered in this patient population given the heterogeneity of pulmonary arterial wall composition and backward wave reflections coming from the proximal pulmonary arterial branches.[2,4] In this study, we have observed nearly two-fold increase in PWV measured at the MPA, similar to a previously reported adult study.[21] Additional studies in the adult literature have reported dramatically decreased RAC along with the MPA compliance and distensibility.[6,28] Other studies have suggested that non-invasive detection of MPA stiffness is an early sign of worsening pulmonary vascular disease correlating with clinically prognostic outcomes, and that stiffness can significantly increase with response to exercise induced stress.[8,29–31] Unfortunately, serial follow-up of paediatric PAH patients by combined catheterization and advanced imaging techniques is challenging due to the invasiveness of cardiac catheterization. Additionally, comprehensive evaluation of pulmonary vascular stiffness using impedance frequency domain analysis along with more simple pulse pressure based metrics (i.e. compliance and distensibility) require catheter derived pressure waveform and are limited for clinical evaluation of pulmonary circulation, especially in children.[32,33] Indeed, the majority of consensus recommendations suggest non-invasive clinical follow-up evaluation by means of echocardiography or CMR.[3] The promising route toward more comprehensive non-invasive characterization of PAH is real-time CMR allowing for high temporal resolution imaging, but this technique is currently applied only in a limited number of institutions due to high post-processing time.[21,34,35]

MPA stiffness and RV afterload

The significant contribution of increased proximal pulmonary vascular stiffness to RV afterload has been demonstrated in both adult and paediatric PAH populations.[4,36–38] In this study, we have shown significant correlations between non-invasive markers of MPA stiffness with volumetric and functional RV indices. Non-invasive evaluation of RV remodelling as a response to elevated afterload has been previously investigated by means of a simplified version of the VVCR (mathematical transform of RV ejection fraction), demonstrating potential for describing disease severity and prediction of clinical outcomes.[20,39,40] Strong association between PWV and RAC with VVCR in our study suggests that critical contribution of proximal stiffness to RV-pulmonary artery axis function can be measured non-invasively in paediatric PAH population and further supports ongoing efforts for finding therapeutic targeting for proximal vascular stiffness.[4,41]

Shear haemodynamics and stiffness

Flow mediated remodelling of pulmonary and systemic vasculature is already recognized phenomenon applicable to broad range of vasculopathies.[7,16] The mechanotransduction driven endothelial and extracellular matrix remodelling in PAH has been described in several *in vitro* and animal studies.[4,17,37,42–44] Similar to systemic circulation, shear mediated response in pulmonary circulation has a spatially heterogeneous response i.e. endothelial cells in the pulmonary artery will have different responsiveness to shear abnormalities than those at the level of pulmonary arterioles.[9,45,46] Furthermore, endothelial response to WSS variations is magnitude and direction specific, with low and oscillatory shear mediating endothelial cell proliferation and activation of the local inflammatory response.[15,16,47] Indeed, in the presented study, we have observed dramatically reduced WSS_{max} and WSS_{TA} along with elevated OSI in the presence of increased MPA stiffness. In the presence of such a condition, the extra-cellular matrix of the MPA has been shown in *in vitro* studies to remodel toward collagen dominant and thus, stiffer, character.[17,48] Importantly,

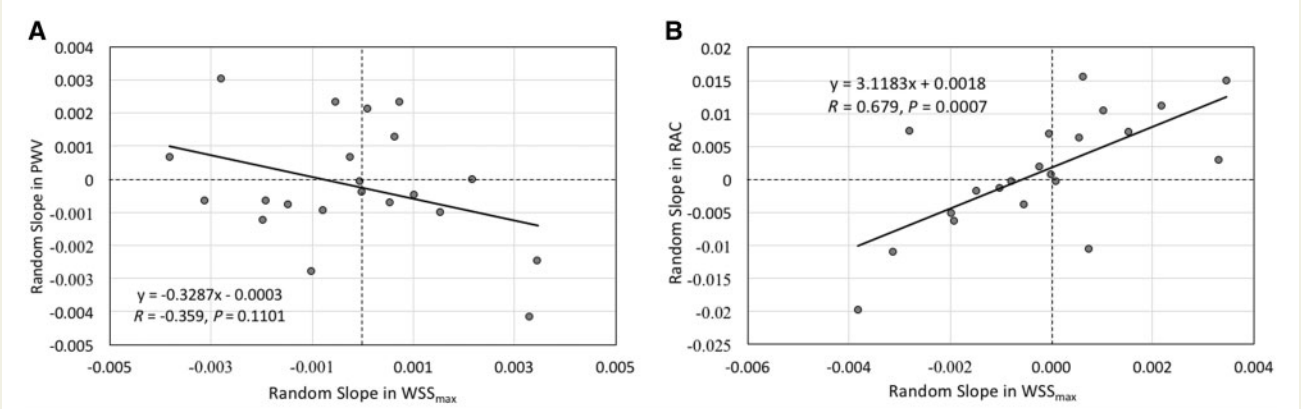

Figure 5 (*A*) Random slope analysis depicting the trend between PWV and WSS_{max} failed to reveal significant relationship between two metrics. (*B*) Contrary, same analysis between the RAC and WSS_{max} revealed significant positive trend.

Table 4 Univariate proportional hazard analysis

	Moderate outcomes (n = 28)		Severe outcomes (n = 13)	
	HR (95% CI)	*P*-value	HR (95% CI)	*P*-value
PWV	3.18 (1.44–7.73)	0.0063*	3.15 (0.98–10.06)	0.0541
RAC	0.75 (0.34–1.62)	0.4672	0.69 (0.18–2.56)	0.5816
WSS_{max}	0.72 (0.32–1.64)	0.4374	0.17 (0.02–1.32)	0.0906
VVCR	1.30 (0.52–3.26)	0.5656	2.70 (0.59–12.39)	0.2003
EF	0.54 (0.24–1.19)	0.1298	0.45 (0.15–1.44)	0.1834
EDVi	1.34 (0.62–2.88)	0.4466	2.25 (0.67–7.51)	0.1844
ESVi	1.23 (0.57–2.64)	0.5876	2.41 (0.65–8.96)	0.1873
SVi	0.75 (0.35–1.63)	0.4748	0.31 (0.09–1.05)	0.0612

Data reported as Cox proportionate hazard ratios with corresponding 95% confidence intervals.
*$P < 0.05$.
EDVi, end-diastolic volume index; EF, ejection fraction; ESVi, end-systolic volume index; *n*, number of adverse events in each category; PWV, pulse wave velocity; RAC, relative area change; SVi, stroke volume index; VVCR, ventricular-vascular coupling ratio; WSSmax, maximum systolic wall shear stress.

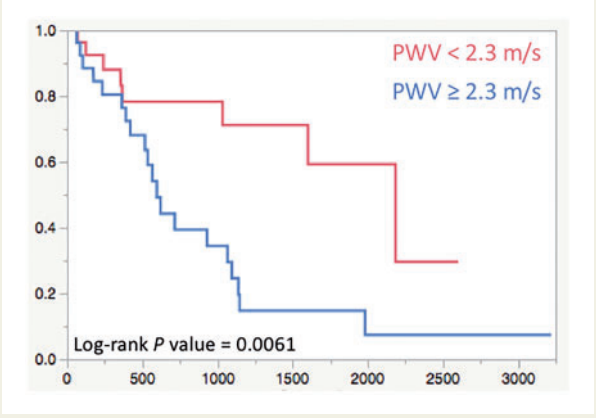

Figure 6 The Kaplan–Meier curve for the PWV measured at the MPA predicting moderate clinical outcomes.

we observed that changes throughout the disease progression in the WSS_{max} correspond to the changes in RAC representing a purely geometric assessment of vascular deformation. Interestingly, the PWV has not shown a significant correlation but was indicative of the corresponding trend. While the major theoretical determinants of WSS, vessel size, was severely enlarged in PAH, one must carry in mind that theoretical WSS as calculated by Haagen–Poisseuille law relationship assumes ideal pipe-flow condition and does not account for pulsatile flow and three-dimensional secondary flow structures (vortices and helices), which are often associated with PAH.[49] Further and more comprehensive studies using four-dimensional flow CMR (4D-Flow CMR) enabling broad three-dimensional WSS analysis will be required to study the relationship between WSS and proximal pulmonary stiffness in paediatric patients. A previous adult study has successfully described reduced WSS assessed by 4D-Flow CMR in the MPA and correlated shear metrics to invasive haemodynamic indices.[49] Other qualitative and quantitative flow haemodynamic metrics of flow disturbances affecting WSS have been correlated with the severity of PAH.[5]

Prognostic value of the MPA stiffness

Several catheterization-derived markers, standard clinical indices, and non-invasive RV echocardiographic and CMR derived specific metrics have been previously shown to be strongly associated with clinically important outcomes in children with PAH. Specifically, MPA stiffness derived indices, reflective of pulsatile load derived by catheterization, have been shown to have good prognostic potential to predict PAH related morbidity and mortality.[50,51] However, none to date have evaluated the prognostic ability of non-invasive imaging stiffness

markers in paediatric PAH population.[34,52] In this study, we considered two different sets of composite outcomes and found that MPA stiffness represented by PWV can be predictive of moderate clinical events. Interestingly, none of the other RV metrics were shown to be predictive of moderate or severe clinical outcomes. We speculate that this is mainly due to smaller number of patients considered for prognostic analysis with respect to previously described large studies and the nature of composite outcomes. Moledina et al has shown significant prognostic potential of RV and left ventricular volumetric indexed measures toward freedom from death or transplantation.[34] Measuring meaningful clinical outcomes in both adult and paediatric populations remains challenging; while more evaluation is needed to find suitable clinical endpoints for this population, composite clinical outcomes made up of less dramatic clinical events should be a priority. Previous work has shown the predictive ability of RAC toward mortality in broad PAH adult populations.[8] Furthermore, invasive stiffness metrics sampled from young children with suspected pulmonary vascular disease has been shown to have prognostic value for PAH severity and the development of PAH in adulthood.[53] In this work, we showed that non-invasively derived PWV, a surrogate for MPA stiffness can predict adverse clinical outcomes.

Limitations

Retrospective analysis of CMR in children with PAH is limiting as there was some heterogeneity in CMR acquisition. The variability in different MRI systems may indeed introduce inter-system variability, however, the previous studies have reported limited effect of different field strength on haemodynamic measurements.[54] The sample size of our PAH cohort limited both baseline and prognostic analysis. This is mainly due to fact that young children (<7 years of age) require sedation for CMR evaluation per institutional protocol. Additionally, severe outcomes are infrequent in the paediatric PAH population lacking a consensus definition of moderate and severe outcomes.[3] Retrospective analysis also limits the ability to coordinate CMR with invasive catheterization, and therefore, clinical decisions made between catheterization and CMR may contribute to altered outcomes. Lastly, our PAH patient population might differ from other centres due to regional factors associated with high altitude. These limitations have been postulated previously as unavoidable in majority of paediatric CMR studies.[22]

A technical limitation is through plane motion of the pulmonary trunk, which may have introduced an error to both PWV (dQ/dA method) and RAC analysis. Furthermore, the PWV measured by flow wave propagation within the proximal pulmonary conduit in children is limited by the spatiotemporal resolution and is more applicable to the aortic stiffness analysis. Herein, we attempted to mitigate all potential errors with backward wave reflections in pulmonary vessels by secluding PWV analysis only to the specific portion of the flow upstroke waveform without evidence of a wave reflection.

Conclusion

Children with PAH have increased pulmonary vascular stiffness as assessed by non-invasive CMR evaluation regardless of PAH aetiology. Metrics of MPA stiffness also correlate with RV volumetric and functional indices implying an important contribution to the RV afterload. MPA stiffness is associated with reduced haemodynamic WSS, and changes in both metrics followed a consistent pattern on follow up CMR. Importantly, we found that PWV measured in the MPA can be predictive of moderate clinical outcomes and therefore may be applied toward CMR follow up evaluation of paediatric PAH patients. The presence of proximal pulmonary vascular stiffness in PAH then should be further considered as therapeutic target in paediatric population.

Funding

This work was supported in part by the The Jayden de Luca Foundation, Actelion ENTELLIGENCE Grant, Children's Hospital Colorado Research Scholar Award, Colorado Clinical Translation Sciences Institute Maternal and Child Pilot Grant, The Frederick and Margaret L. Weyerhaeuser Foundation, NIH grants R01HL114753, U01HL121518, NHLBI U01 HL12118, NHLBI RO1 HL085703, NHLBI RO1 HL68702, K25-HL094749, and by NIH/NCATS Colorado CTSA Grant Number UL1 TR001082.

Conflict of interest: none declared.

References

1. Tozzi CA, Christiansen DL, Poiani GJ, Riley DJ. Excess collagen in hypertensive pulmonary arteries decreases vascular distensibility. *Am J Respir Crit Care Med* 1994;**149**:1317–26.
2. Stenmark KR, Fagan KA, Frid MG. Hypoxia-induced pulmonary vascular remodeling: cellular and molecular mechanisms. *Circ Res* 2006;**99**:675–91.
3. Abman SH, Hansmann G, Archer SL, Ivy DD, Adatia I, Chung WK *et al*. Pediatric pulmonary hypertension. *Circulation* 2015;**132**:2037–99.
4. Schäfer M, Myers C, Brown RD, Frid MG, Tan W, Hunter K *et al*. Pulmonary arterial stiffness: toward a new paradigm in pulmonary arterial hypertension pathophysiology and assessment. *Curr Hypertens Rep* 2016;**18**:4.
5. Reiter G, Reiter U, Kovacs G, Kainz B, Schmidt K, Maier R *et al*. Magnetic resonance-derived 3-dimensional blood flow patterns in the main pulmonary artery as a marker of pulmonary hypertension and a measure of elevated mean pulmonary arterial pressure. *Circ Cardiovasc Imaging* 2008;**1**:23–30.
6. Sanz J, Kariisa M, Dellegrottaglie S, Prat-González S, Garcia MJ, Fuster V *et al*. Evaluation of pulmonary artery stiffness in pulmonary hypertension with cardiac magnetic resonance. *JACC Cardiovasc Imaging* 2009;**2**:286–95.
7. Swift AJ, Rajaram S, Hurdman J, Hill C, Davies C, Sproson TW *et al*. Noninvasive estimation of pa pressure, flow, and resistance with CMR imaging: derivation and prospective validation study from the aspire registry. *JACC Cardiovasc Imaging* 2013;**6**:1036–47.
8. Swift AJ, Rajaram S, Condliffe R, Capener D, Hurdman J, Elliot C *et al*. Pulmonary artery relative area change detects mild elevations in pulmonary vascular resistance and predicts adverse outcome in pulmonary hypertension. *Invest Radiol* 2012;**47**:571–7.
9. Szulcek R, Happé CM, Rol N, Fontijn RD, Dickhoff C, Hartemink KJ *et al*. Delayed microvascular shear-adaptation in pulmonary arterial hypertension: role of PECAM-1 cleavage. *Am J Respir Crit Care Med* 2016;**33**:1–58.
10. Guzzardi DG, Barker AJ, Ooij P, van Malaisrie SC, Puthumana JJ, Belke DD *et al*. Valve-related hemodynamics mediate human bicuspid aortopathy. *J Am Coll Cardiol* 2015;**66**:892–900.
11. Barst RJ, Ertel SI, Beghetti M, Ivy DD. Pulmonary arterial hypertension: a comparison between children and adults. *Eur Respir J* 2011;**37**:665–77.
12. Hopper RK, Abman SH, Ivy DD. Persistent challenges in pediatric pulmonary hypertension. *Chest* 2016;**150**:226–36.
13. Truong U, Fonseca B, Dunning J, Burgett S, Lanning C, Ivy DD *et al*. Wall shear stress measured by phase contrast cardiovascular magnetic resonance in children and adolescents with pulmonary arterial hypertension. *J Cardiovasc Magn Reson* 2013;**15**:81.
14. Schäfer M, Ivy DD, Barker AJ, Kheyfets V, Shandas R, Abman SH *et al*. Characterization of CMR-derived haemodynamic data in children with pulmonary arterial hypertension. *Eur Heart J Cardiovasc Imaging* 2017;**18**:424–31.
15. Davies PF. Hemodynamic shear stress and the endothelium in cardiovascular pathophysiology. *Nat Rev Cardiol* 2009;**6**:16–26.
16. Malek AM, Alper SL, Izumo S. Hemodynamic shear stress and its role in atherosclerosis. *J Am Med Assoc* 1999;**282**:2035–42.

17. Li M, Tan Y, Stenmark KR, Tan W. High pulsatility flow induces acute endothelial inflammation through overpolarizing cells to activate NF-kB. *Cardiovasc Eng Technol* 2013;**4**:26–38.
18. Del Cerro MJ, Moledina S, Haworth SG, Ivy D, Dabbagh M, Al Banjar H *et al*. Cardiac catheterization in children with pulmonary hypertensive vascular disease: consensus statement from the Pulmonary Vascular Research Institute, Pediatric and Congenital Heart Disease Task Forces. *Pulm Circ* 2016;**6**:118–25.
19. Nayak KS, Nielsen JF, Bernstein MA, Markl M, D. Gatehouse P, M. Botnar R *et al*. Cardiovascular magnetic resonance phase contrast imaging. *J Cardiovasc Magn Reson* 2015;**17**:71.
20. Sanz J, Nair A, Ferna L, Garcı A, Mirelis G, Sawit ST *et al*. Right ventriculo-arterial coupling in pulmonary hypertension: a magnetic resonance study. *Heart* 2012;**98**:238–44.
21. Quail MA, Knight DS, Steeden JA, Taelman L, Moledina S, Taylor AM *et al*. Noninvasive pulmonary artery wave intensity analysis in pulmonary hypertension. *Am J Physiol Heart Circ Physiol* 2015;**308**:H1603–11.
22. Schäfer M, Ivy DD, Abman SH, Barker AJ, Browne LP, Fonseca B *et al*. Apparent aortic stiffness in children with pulmonary arterial hypertension. *Circ Cardiovasc Imaging* 2017;**10**:e005817.
23. Wentland AL, Grist TM, Wieben O. Review of MRI-based measurements of pulse wave velocity: a biomarker of arterial stiffness. *Cardiovasc Diagn Ther* 2014;**4**:193–206.
24. Ku DN, Giddens DP, Zarins CK, Glagov S. Pulsatile flow and atherosclerosis in the human carotid bifurcation. Positive correlation between plaque location and low oscillating shear stress. *Arteriosclerosis* 1985;**5**:293–302.
25. Nordgaard H, Swillens A, Nordhaug D, Kirkeby-Garstad I, Loo D, Van Vitale N *et al*. Impact of competitive flow on wall shear stress in coronary surgery: computational fluid dynamics of a LIMA-LAD model. *Cardiovasc Res* 2010;**88**:512–9.
26. Bernus A, Wagner BD, Accurso F, Doran A, Kaess H, Ivy DD. Brain natriuretic peptide levels in managing pediatric patients with pulmonary arterial hypertension. *Chest* 2009;**135**:745–51.
27. Quail MA, Short R, Pandya B, Steeden JA, Khushnood A, Taylor AM *et al*. Abnormal wave reflections and left ventricular hypertrophy late after coarctation of the aorta repair. *Hypertension* 2017;**69**:501–9.
28. Lankhaar JW, Westerhof N, Faes TJC, Gan CTJ, Marques KM, Boonstra A *et al*. Pulmonary vascular resistance and compliance stay inversely related during treatment of pulmonary hypertension. *Eur Heart J* 2008;**29**:1688–95.
29. Forouzan O, Warczytowa J, Wieben O, François CJ, Chesler NC. Non-invasive measurement using cardiovascular magnetic resonance of changes in pulmonary artery stiffness with exercise. *J Cardiovasc Magn Reson* 2015;**17**:109.
30. Gan CTJ, Lankhaar JW, Westerhof N, Marcus JT, Becker A, Twisk JWR *et al*. Noninvasively assessed pulmonary artery stiffness predicts mortality in pulmonary arterial hypertension. *Chest* 2007;**132**:1906–12.
31. Reeves JT, Linehan JH, Stenmark KR. Distensibility of the normal human lung circulation during exercise. *Am J Physiol Lung Cell Mol Physiol* 2005;**288**:L419–25.
32. Westerhof N, Segers P, Westerhof BE. Wave separation, wave intensity, the reservoir-wave concept, and the instantaneous wave-free ratio: presumptions and principles. *Hypertension* 2015;**66**:93–8.
33. Saouti N, Westerhof N, Postmus PE, Vonk-Noordegraaf A. The arterial load in pulmonary hypertension. *Eur Respir Rev* 2010;**19**:197–203.
34. Moledina S, Pandya B, Bartsota M, Mortensen KH, McMillan M, Quyam S *et al*. Prognostic significance of cardiac magnetic resonance imaging in children with pulmonary hypertension. *Circ Cardiovasc Imaging* 2013;**6**:407–14.
35. Pandya B, Quail MA, Steeden JA, McKee A, Odille F, Taylor AM *et al*. Real-time magnetic resonance assessment of septal curvature accurately tracks acute hemodynamic changes in pediatric pulmonary hypertension. *Circ Cardiovasc Imaging* 2014;**7**:706–13.
36. Vonk Noordegraaf A, Westerhof BE, Westerhof N. The relationship between the right ventricle and its load in pulmonary hypertension. *J Am Coll Cardiol* 2017;**69**:236–43.
37. Tan Y, Tseng PO, Wang D, Zhang H, Hunter K, Hertzberg J *et al*. Stiffening-induced high pulsatility flow activates endothelial inflammation via a TLR2/NF-κB pathway. *PLoS One* 2014;**9**:e102195–14.
38. Hunter KS, Lee P, Lanning CJ, Ivy DD, Kirby KS, Claussen LR *et al*. Pulmonary vascular input impedance is a combined measure of pulmonary vascular resistance and stiffness and predicts clinical outcomes better than PVR alone in pediatric patients with pulmonary hypertension with pulmonary hypertension. *Am Heart J* 2008;**155**:166–74.
39. Vanderpool RR, Pinsky MR, Naeije R, Deible C, Kosaraju V, Bunner C *et al*. RV-pulmonary arterial coupling predicts outcome in patients referred for pulmonary hypertension. *Heart* 2015;**101**:37–43.
40. Vanderpool RR, Rischard F, Naeije R, Hunter K, Simon MA. Simple functional imaging of the right ventricle in pulmonary hypertension: can right ventricular ejection fraction be improved? *Int J Cardiol* 2016;**223**:93–4.
41. Thenappan T, Prins KW, Pritzker MR, Scandurra J, Volmers K, Weir EK. The critical role of pulmonary arterial compliance in pulmonary hypertension. *Ann Am Thorac Soc* 2016;**13**:276–84.
42. Scott D, Tan Y, Shandas R, Stenmark KR, Tan W. High pulsatility flow stimulates smooth muscle cell hypertrophy and contractile protein expression. *Am J Physiol Lung Cell Mol Physiol* 2012;70–81.
43. Budhiraja R, Tuder RM, Hassoun PM. Endothelial dysfunction in pulmonary hypertension. *Circulation* 2004;**109**:159–65.
44. Hassoun PM, Mouthon L, Barberà J. A, Eddahibi S, Flores SC, Grimminger F *et al*. Inflammation, growth factors, and pulmonary vascular remodeling. *J Am Coll Cardiol* 2009;**54**:S10–9.
45. Bloodworth NC, West JD, Merryman WD. Microvessel mechanobiology in pulmonary arterial hypertension. *Hypertension* 2015;**65**:483–9.
46. Gerhold KA, Schwartz MA. Ion channels in endothelial responses to fluid shear stress. *Physiology (Bethesda)* 2016;**31**:359–69.
47. Chiu JJ, Chien S. Effects of disturbed flow on vascular endothelium: pathophysiological basis and clinical perspectives. *Physiol Rev* 2011;**91**:327–87.
48. Tan W, Madhavan K, Hunter KS, Park D, Stenmark KR. Vascular stiffening in pulmonary hypertension: cause or consequence? (2013 Grover Conference series). *Pulm Circ* 2014;**4**:560–80.
49. Schafer M, Kheyfets VO, Schroeder JD, Dunning J, Shandas R, Buckner JK *et al*. Main pulmonary arterial wall shear stress correlates with invasive hemodynamics and stiffness in pulmonary hypertension. *Pulm Circ* 2016;**6**:37–45.
50. Takatsuki S, Nakayama T, Ikehara S, Matsuura H, Ivy DD, Saji T. Pulmonary arterial capacitance index is a strong predictor for adverse outcome in children with idiopathic and heritable pulmonary arterial hypertension. *J Pediatr* 2017;**180**:75–9.e2.
51. Sajan I, Manlhiot C, Reyes J, McCrindle BW, Humpl T, Friedberg MK. Pulmonary arterial capacitance in children with idiopathic pulmonary arterial hypertension and pulmonary arterial hypertension associated with congenital heart disease: relation to pulmonary vascular resistance, exercise capacity, and survival. *Am Heart J* 2011;**162**:562–8.
52. Ploegstra MJ, Arjaans S, Zijlstra WMH, Douwes JM, Vissia-Kazemier TR, Roofthooft MTR *et al*. Clinical worsening as composite study end point in pediatric pulmonary arterial hypertension. *Chest* 2015;**148**:655–66.
53. Ploegstra MJ, Brokelman JGM, Roos-Hesselink JW, Douwes JM, Osch-Gevers LM, van, Hoendermis ES *et al*. Pulmonary arterial stiffness indices assessed by intravascular ultrasound in children with early pulmonary vascular disease: prediction of advanced disease and mortality during 20-year follow-up. *Eur Heart J Cardiovasc Imaging* 2017;**184**:198–207.
54. Barker AJ, Roldán-Alzate A, Entezari P, Shah SJ, Chesler NC, Wieben O *et al*. Four-dimensional flow assessment of pulmonary artery flow and wall shear stress in adult pulmonary arterial hypertension: results from two institutions. *Magn Reson Med* 2015;**73**:1904–13.